Performance evaluation of PAM-4 modulated Hermite-Gaussian mode division multiplexed underwater optical wireless communication system under Jerlov water conditions

AMIT GROVER[1], MEHTAB SINGH[2,*], KARAMJEET SINGH[3], SOMIA A. ABD EL-MOTTALEB[4], AMMAR ARMGHAN[5], TANVIR KAUR[6]
[1]*Department of Electronics and Communication Engineering, Shaheed Bhagat Singh State University, Ferozepur, Punjab, India*
[2]*Department of Electronics and Communication Engineering, Chandigarh University, Mohali-140413, Punjab, India*
[3]*Department of Electronics and Communication Engineering, Shaheed Bhagat Singh State University, Ferozepur, Punjab, India*
[4]*Alexandria Higher Institute of Engineering and Technology, Alexandria, Egypt*
[5]*Department of Electrical Engineering, College of Engineering, Jouf University, Sakaka 72388, Saudi Arabia*
[6]*Amazon Web Services, USA*

This paper presents the design and performance evaluation of a mode division multiplexing (MDM)-based underwater optical wireless communication (UOWC) system employing Hermite-Gaussian (HG) modes and four-level pulse amplitude modulation (PAM-4) signaling. The system utilizes four orthogonal HG modes (HG_0^0, HG_1^0, HG_0^1, and HG_1^1) to achieve an aggregated transmission capacity of 80 Gbps (20 Gbps per mode). The optical link performance is analyzed over five distinct Jerlov water types—JI, JIA, JIB, JII, and JIII—considering the impact of increasing propagation distance on bit error rate (BER), error vector magnitude (EVM), and eye diagram characteristics. The simulation results indicate that the proposed HG-MDM-UOWC system supports reliable transmission distances of approximately 65 m, 51 m, 28.5 m, 13.2 m, and 4.75 m for JI, JIA, JIB, JII, and JIII water types respectively, at the forward error correction (FEC) threshold. Among the evaluated scenarios, JI water demonstrates the best performance with minimal EVM degradation and clear eye openings across all HG channels. The findings confirm that spatial mode multiplexing through orthogonal HG beams significantly enhances data throughput in UOWC systems, though performance strongly depends on water clarity and scattering characteristics.

(Received October 20, 2025; accepted February 2, 2026)

Keywords: Underwater optical wireless communication, Mode division multiplexing, Hermite Gaussian modes, PAM-4, Propagation range

1. Introduction

The growing demand for broadband connectivity and real-time data transfer in underwater environments has intensified the global research focus on underwater wireless communication (UWC) technologies [1]. Applications such as oceanographic data collection, marine life monitoring, offshore infrastructure inspection, underwater vehicle coordination, and defense surveillance rely heavily on efficient underwater communication systems [2, 3]. Traditional underwater communication methods, primarily acoustic and radio frequency (RF)-based systems, face fundamental constraints that limit their suitability for high-capacity data-driven operations [4]. Acoustic communication, despite offering long-range connectivity up to several kilometers, suffers from extremely low bandwidth (<100 kHz), high latency (propagation speed ≈ 1500 m/s), and strong susceptibility to Doppler and multipath distortions [5]. Radio frequency communication, on the other hand, is severely attenuated in conductive seawater, restricting its range to only a few meters, even with powerful transmitters. These limitations have created a compelling need for high-speed, energy-efficient alternatives—leading to the emergence of underwater optical wireless communication (UOWC) as a promising solution.

UOWC exploits visible or near-infrared optical wavelengths to realize broadband, low-latency, and energy-efficient communication links in underwater environments. By leveraging the vast unlicensed optical spectrum, UOWC systems can achieve data transmission rates in the order of tens to hundreds of gigabits per second (Gbps) over distances of several tens of meters under favorable conditions [6, 7]. Optical communication underwater exhibits several inherent advantages: high directionality, reduced latency, immunity to electromagnetic interference, and compact transceiver design. However, its practical realization is hindered by significant physical impairments such as absorption,

scattering, and turbulence-induced beam wandering—factors that are strongly dependent on the optical properties of the water medium [8 – 11]. These properties vary drastically across Jerlov's water classification, which categorizes water into distinct types (JI to JIII) based on clarity and scattering coefficients. Clear oceanic waters (JI, JIA, JIB) enable longer communication ranges with relatively low extinction coefficients, whereas turbid coastal waters (JII and JIII) exhibit severe attenuation that restricts the viable communication distance [12].

Recent advancements in modulation and multiplexing techniques have been pivotal in enhancing the data rates and robustness of UOWC systems. Conventional intensity modulation and direct detection (IM/DD) schemes such as on–off keying (OOK) and pulse position modulation (PPM) have been widely investigated [13, 14]; however, their spectral efficiency and tolerance to underwater impairments remain limited. To address these challenges, pulse amplitude modulation (PAM) [15], quadrature amplitude modulation (QAM) [16], orthogonal frequency division multiplexing (OFDM) [17], and spatial multiplexing schemes [18] have been proposed. Among these, PAM-4 has gained significant attention owing to its simplicity, power efficiency, and improved spectral utilization compared to binary modulation formats. The use of PAM-4 can double the data rate without requiring additional bandwidth, making it particularly suitable for high-speed underwater links constrained by physical channel limitations. Recent studies have validated multi-level formats in UOWC. The authors in [19] demonstrated 4/8-QAM outperforming OOK/ quadrature phase shift keying (QPSK)/4-PAM in pure/seawater via bit error rate (BER) analysis at 405 nm LED, emphasizing QAM robustness. Similarly, the work in [20] compared OOK/pulse position modulation (PPM)/QPSK/64-QAM across pure/turbid waters at 520 nm, revealing trade-offs in range (OOK longest) vs. capacity (64-QAM highest) under turbulence. These affirm PAM-4's balance of efficiency and practicality for our HG-MDM system. Compared to conventional non-return-to-zero (NRZ) and return-to-zero (RZ) formats, PAM-4 offers key merits including doubled spectral efficiency (2 bits/symbol vs. 1 bit/symbol), enabling higher data rates within the same bandwidth-constrained underwater channel; reduced electrical bandwidth requirements (half of NRZ for equivalent bit rate); and lower peak-to-average power ratio (PAPR) for improved transmitter efficiency in battery-limited UOWC nodes. While PAM-4 exhibits slightly reduced noise tolerance per level compared to binary schemes, its integration with forward error correction (FEC) effectively mitigates this in practical systems, as demonstrated in our HG-MDM architecture.

Parallel to modulation advances, mode division multiplexing (MDM) has emerged as an efficient multiplexing strategy to expand UOWC capacity by utilizing distinct spatial modes of light as independent transmission channels [21]. In MDM, mutually orthogonal spatial modes—such as Hermite–Gaussian (HG), Laguerre–Gaussian (LG), or Bessel modes—are used to carry separate data streams simultaneously within the same wavelength and polarization state. This technique effectively multiplies the capacity of a single optical channel while maintaining orthogonality between beams, thus minimizing intermodal crosstalk. Although MDM has been extensively used in terrestrial fiber and free-space optics (FSO) systems, its adaptation to underwater environments is relatively recent and poses unique challenges due to mode distortion and scattering-induced coupling in turbid waters. HG modes, in particular, offer favorable characteristics for mode multiplexed UOWC links. They form a complete orthogonal set of solutions to the paraxial wave equation in Cartesian coordinates and can be generated using simple optical setups. HG modes exhibit discrete intensity distributions that are resilient to beam wander and possess better spatial confinement compared to vortex-based LG modes. Recent research has highlighted their potential for robust underwater transmission due to their symmetric beam profiles and reduced sensitivity to turbulence-induced distortions. HG modes are specifically selected over alternatives like Laguerre-Gaussian (LG), orbital angular momentum (OAM) and linearly polarized (LP) modes due to: (i) Cartesian rectangular symmetry aligning with detector arrays for simpler multiplexing/demultiplexing via spatial light modulators (SLMs)/cylindrical lenses; (ii) complete orthogonal basis with lower scattering-induced coupling in turbid waters; (iii) easier cavity excitation without phase singularities, enhancing robustness to underwater beam wander vs. OAM fragility. These advantages make HG ideal for practical, high-capacity UOWC spatial multiplexing. The orthogonality among HG modes enables efficient multiplexing and demultiplexing processes using SLMs or mode sorters, making them practical candidates for high-capacity underwater optical systems.

Despite these advantages, significant research gaps persist in quantifying the performance of HG-mode multiplexed UOWC systems under realistic oceanic conditions. Most reported works have focused on either single-mode or dual-mode transmissions with relatively low data rates (<10 Gbps), and the integration of multichannel MDM with advanced modulation remains underexplored for underwater optical domains. Therefore, evaluating the joint performance of PAM-4 modulation with HG-mode MDM over multiple Jerlov types provides a novel framework to understand the trade-offs between range, data rate, and signal quality in underwater optical links.

In this study, a comprehensive 80 Gbps MDM-based UOWC system using four orthogonal Hermite–Gaussian modes (HG_0^0, HG_1^0, HG_0^1, and HG_1^1) is designed and numerically analyzed. Each mode transmits a 20 Gbps binary data stream modulated using PAM-4. The novelty of this work lies in the combined implementation of HG-mode-based spatial multiplexing and PAM-4 modulation for high-speed UOWC links across standardized Jerlov water classes. System description is given in Section 2, followed by results and discussion in Section 3 and conclusion in Section 4.

2. System setup

Fig. 1 shows the schematic of the proposed PAM-4-based HG-MDM-UOWC transmission system setup schematic designed and evaluated using Optisystem v.22.0 software.

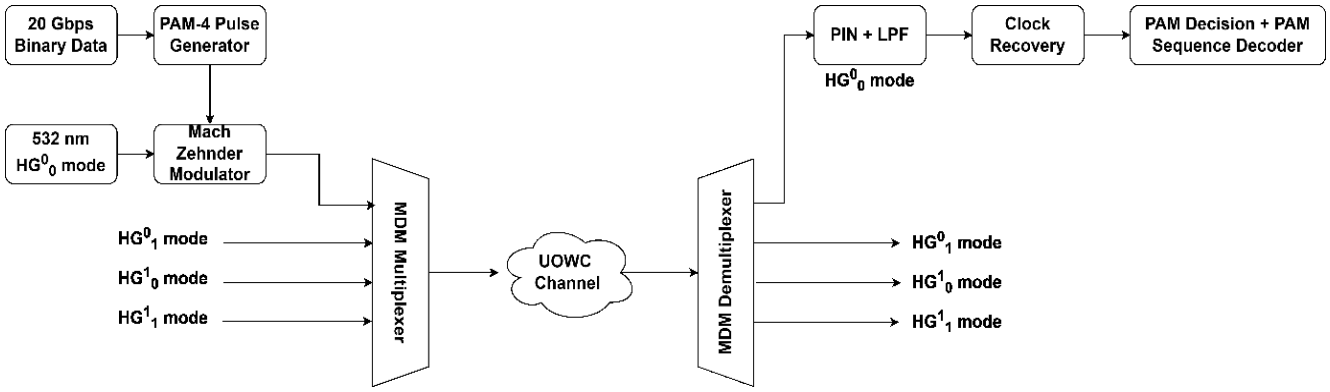

Fig. 1. Schematic of the proposed PAM-4-based HG-MDM-UOWC transmission system

The proposed UOWC system architecture implements parallel high-speed transmission using HG spatial modes and PAM-4 signals, optimized for the underwater optical channel as shown in the Fig. 1. At the transmitter side, each of four independent 20 Gbps binary data streams is assigned to a unique HG mode channel (HG_0^0, HG_1^0, HG_0^1, and HG_1^1). The spatial profiles of HG beams are shown in Fig. 2.

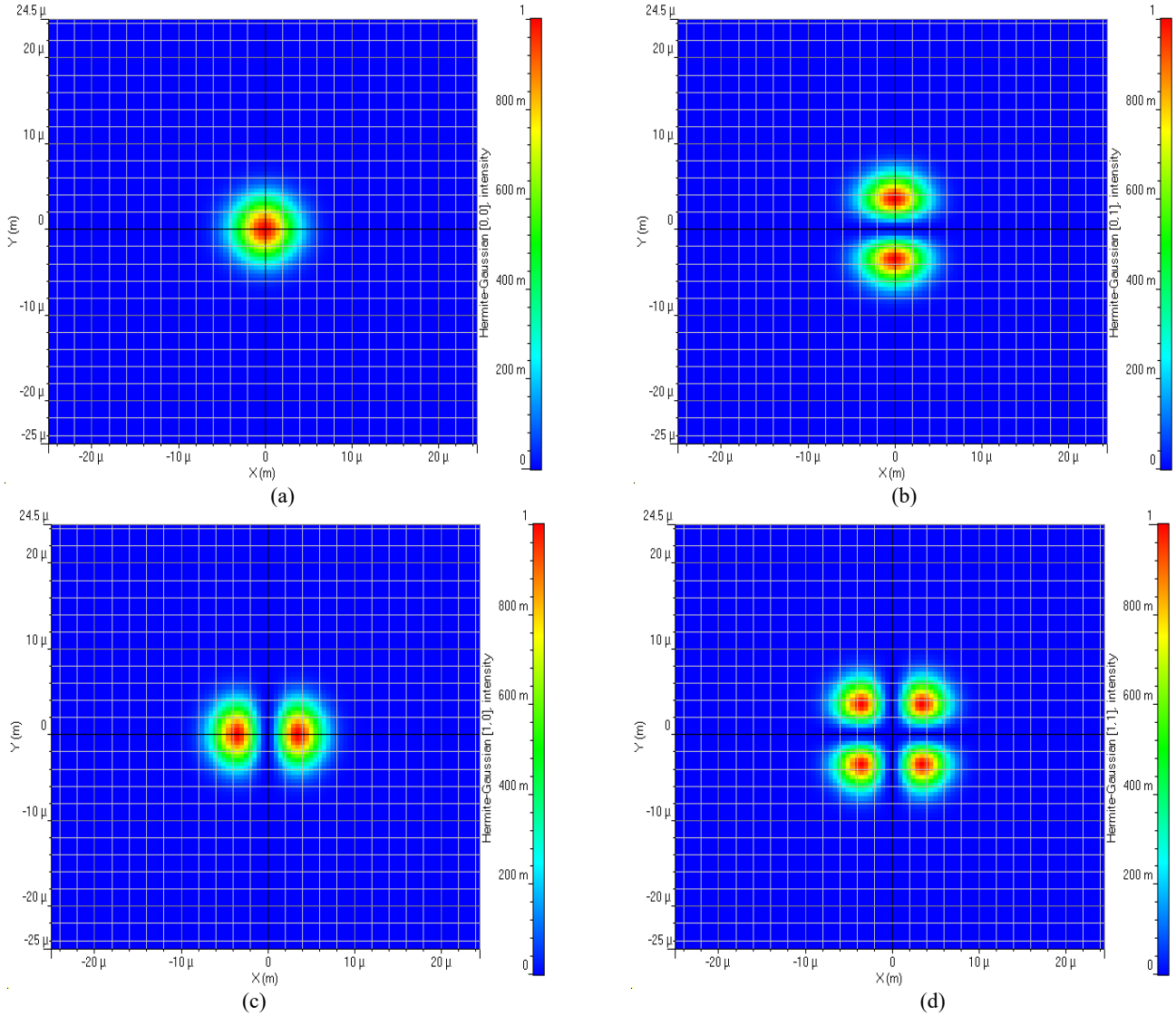

Fig. 2. Spatial profile of (a) HG_0^0 beam (b) HG_1^0 beam (c) HG_0^1 beam (d) HG_1^1 beam (colour online)

HG beam can mathematically be described as [22]:

$$\psi_{m,n}(r,\varphi) = H_m\left(\frac{\sqrt{2}x}{w_{ox}}\right)\exp\left(-\frac{x^2}{w_{0x}^2}\right)H_n\left(\frac{\sqrt{2}y}{w_{oy}}\right)\exp\left(-\frac{y^2}{w_{0y}^2}\right)\exp\left(j\frac{\pi y^2}{\lambda R_{oy}}\right) \quad (1)$$

where m and n represent the mode dependency on X-axis and Y-axis respectively, R represent the radius of curvature and w_o denotes the spot size. H_m and H_n represent the Hermite polynomials. The binary data are first processed by dedicated PAM-4 pulse generators, producing four-level electrical signals with enhanced spectral efficiency. For optical modulation, a Mach–Zehnder modulator is used to impress the PAM-4 signal onto the corresponding HG mode's optical carrier at 532 nm wavelength. The generation of distinct HG mode beams (including the fundamental and first-order Cartesian modes) ensures spatial orthogonality, minimizing modal crosstalk and allowing simultaneous data transmission over shared underwater media. Each HG modulated beam thus represents a separate logical channel capable of supporting 20 Gbps throughput. These four optical HG beams are then combined using an MDM multiplexer. The MDM multiplexer physically aligns and launches the beams into the underwater channel while preserving mode purity and minimizing alignment losses. The multiplexed aggregate data stream, now at 80 Gbps, propagates through the underwater medium, encountering scattering, absorption, and turbulence effects specific to the Jerlov water type being studied. The UOWC transmission can mathematically be presented as [23]:

$$P_R = P_T\eta_T\eta_R\exp[-c(\lambda)\frac{d}{\cos\theta}]\frac{A_{Rec}\cos\theta}{2\pi d^2[1-\cos\theta_0]} \quad (2)$$

Here, P_R and P_T denoted the optical received and transmitted power levels respectively, η_T and η_R represent the transmitter and receiver optical efficiency, d denotes the perpendicular distance between transmitter and receiver plane, A_{Rec} denotes the area of the receiver plane, θ_0 represents the beam divergence angle of the laser diode, and θ is perpendicular angle between the plane of receiver and the trajectory of transmitter-receiver. $c(\lambda)$ denotes the total attenuation coefficient of UOWC medium and is given as [23]:

$$c(\lambda) = c_a(\lambda) + c_s(\lambda) \quad (3)$$

Here $c_a(\lambda)$ denotes the absorption coefficient and $c_s(\lambda)$ denotes the scattering coefficient of UOWC medium. Table 1 shows the absorption and scattering coefficients of different Jerlov water types. The simulation setting used in this work are given in Table 2.

Table 1. Attenuation coefficient for different Jerlov water types [24]

Water type	$c_a(\lambda)$ (m^{-1})	$c_s(\lambda)$ (m^{-1})	$c(\lambda)$ (m^{-1})
JI	0.0464	0.0112	0.0576
JIA	0.0491	0.0334	0.0825
JIB	0.0595	0.1300	0.1895
JII	0.1152	0.4145	0.5297
JIII	0.8451	1.0547	1.8998

Table 2. UOWC link parameters [25]

Parameter	**Symbol**	**Value**	**Unit**
Wavelength	λ	532	nm
Laser power	P_T	10	dBm
Number of spatial beams	-	4	-
Beams used	-	$HG_0^0, HG_1^0, HG_0^1,$ and HG_1^1	-
Laser Linewidth	Δv	100e-012	MHz
Data-rate	R_b	20	Gbps
Baud-rate	R_s	10	Gbps
Transmitter-diameter	D_T	5	cm
Receiver-diameter	D_R	20	cm
Transmitter Optics efficiency	η_T	90	%
Receiver Optics efficiency	η_R	90	%
Beam divergence angle	θ_0	2	mrad
Modulation Schemes	-	PAM-4	-
PIN-responsivity	$\Re$	0.8	A/W

At the receiver, the MDM demultiplexer spatially separates the received composite beam into its original HG mode components, effectively reconstructing mode-isolated data channels even after underwater propagation impairments. Each channel is directed to a PIN photodiode for optical-electrical conversion, followed by low-pass filtering to eliminate high-frequency noise and intersymbol interference. The PAM-4 signals are then fed into a clock recovery module to stabilize timing and enable accurate sampling. Subsequently, PAM decision circuitry demodulates the recovered waveform and a sequence decoder reconstructs the original binary data. This multi-stage detection architecture ensures reliable, error-resilient data recovery for each HG mode, enabling comprehensive BER and Error Vector Magnitude (EVM) analysis across all spatial channels. The system's modular structure

guarantees scalability, allowing additional modes or higher-order PAM formats to further increase system capacity. The spatial orthogonality inherent to HG modes supports robust multiplexing under varying underwater

3. Results and discussion

In this section, the performance evaluation results of the proposed 80 Gbps PAM-4-based HG-MDM-UOWC transmission system are reported and discussed. We have considered log(BER) and EVM as metrics for performance analysis. EVM measures the deviation between ideal and actual constellation points in digital modulation schemes used in optical links, quantifying signal quality from impairments like attenuation or turbulence. EVM for PAM-4 signals measures the deviation between received symbols and their ideal voltage levels across the four amplitude states. It is calculated by comparing the measured signal against a reference PAM-4 constellation on a per-symbol basis, then taking the RMS average of these errors normalized to the ideal signal's power. Fig. 3 (a) and (b) report the EVM% and log(BER) plots respectively versus increasing UOWC range using the proposed system under JI water type conditions. The results report that the EVM is computed as 17.44, 22.24, and 27.25 % for Channel 1-HG_0^0 mode; 17.21, 22.48, and 28.90 % for Channel 2-HG_1^0 mode; 16.64, 21.79, and 29.02 % for Channel 3-HG_0^1 mode; and 17.79, 23.01, and 27.72 % for Channel 4-HG_1^1 mode at 65, 72.5, and 80 m UOWC range respectively. Similarly, log(BER) is reported as -3.01, -1.43, and -0.85 for Channel 1-HG_0^0 mode; -2.79, -1.47, and -0.88 for Channel 2-HG_1^0 mode; -2.46, -1.54, and -0.87 for Channel 3-HG_0^1 mode; and -2.53, -1.40, and -0.83 for Channel 4-HG_1^1 mode at 65, 72.5, and 80 m UOWC range respectively. The results report that increasing UOWC transmission range has a degrading effect on the performance of the proposed system in terms of quality of the received optical beams. The proposed 80 Gbps PAM-4-based HG-MDM-UOWC transmission system demonstrates reliable 65 m transmission for JI water type conditions with good EVM ($\leq$ 17.5%) and log(BER) (~ -2.42 i.e. FEC threshold limit) commonly adopted in high-speed optical systems (e.g., 7% overhead Reed-Solomon (RS) codes as per ITU-T G.975.1) [26]. This pre-FEC limit ensures post-FEC BER < 10^{-12} after decoding, balancing coding gain and overhead for practical UOWC deployment. Fig. 4 (a) – (e) report the eye diagrams of the received signal at 65 m UOWC range under JI water conditions using the proposed system. Clear eye diagrams with wide eye opening and distinct levels demonstrate reliable 80 Gbps-65 m transmission under JI conditions.

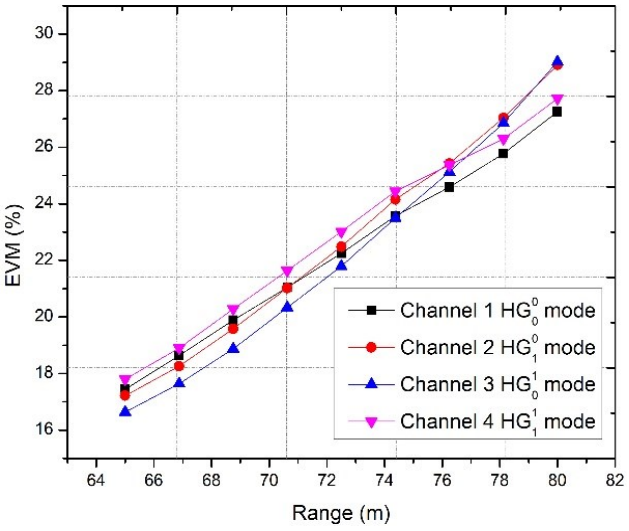

(a)

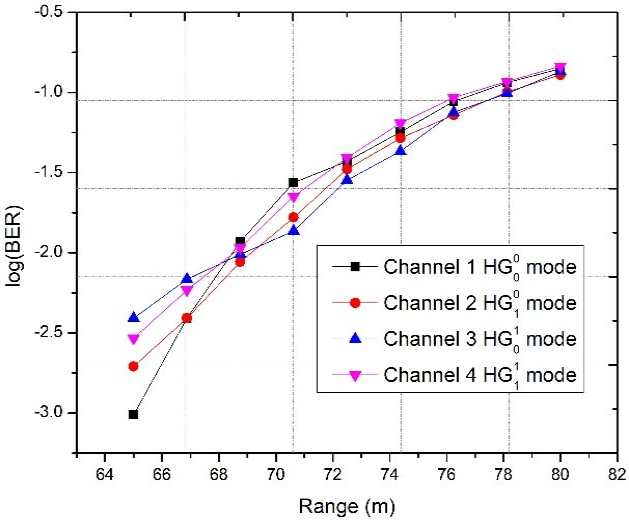

(b)

Fig. 3. (a) EVM% (b) log(BER) versus UOWC range for JI water type (colour online)

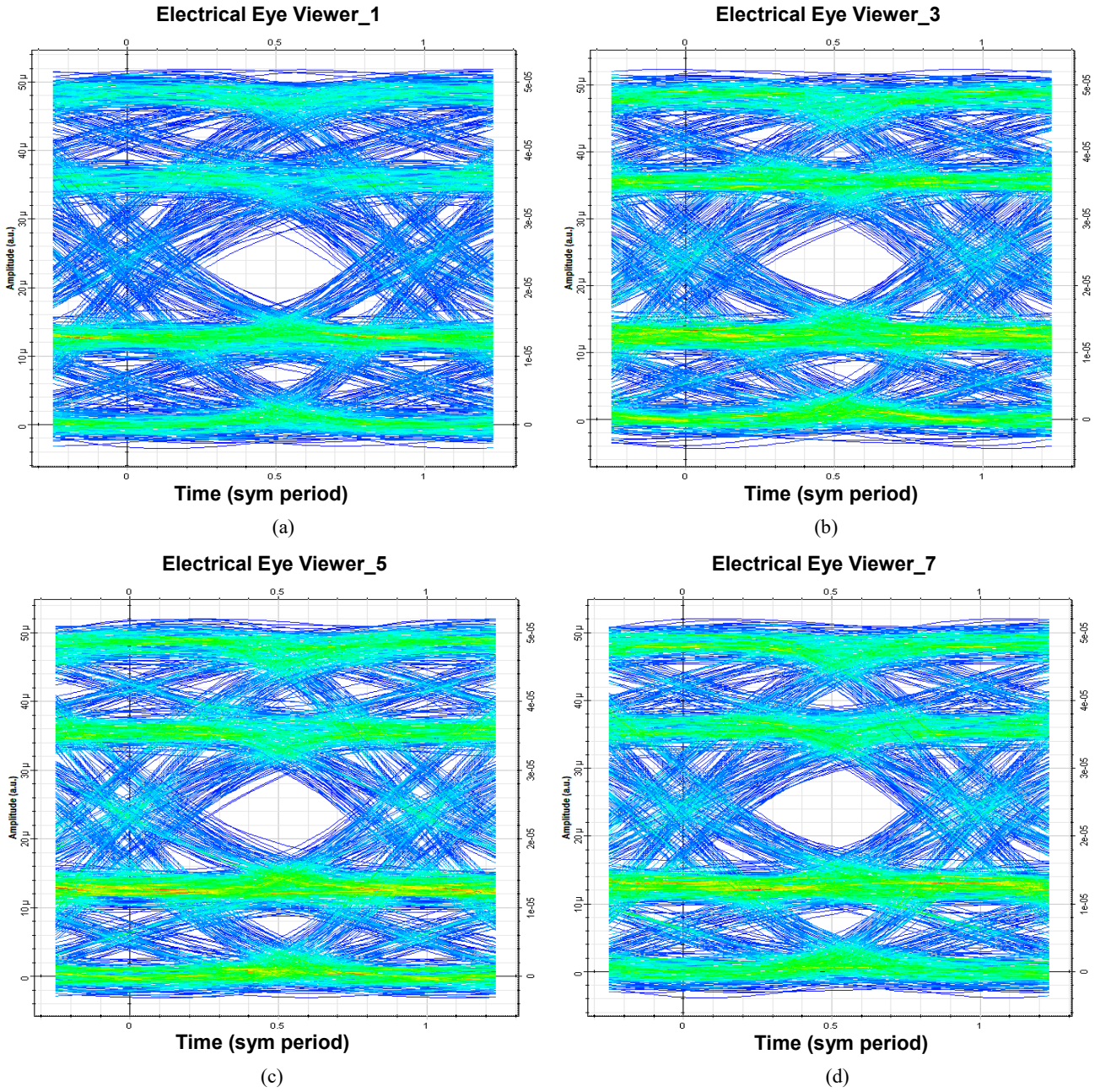

Fig. 4. Eye diagrams for (a) Channel 1-HG_0^0 mode (b) Channel 2-HG_1^0 mode (c) Channel 3-HG_0^1 mode (d) Channel 4-HG_1^1 mode at 65 m under JI water type (colour online)

Fig. 5 (a) and (b) report the EVM% and log(BER) plots respectively versus increasing UOWC range using the proposed system under JIA water type conditions. The results report that the EVM is computed as 17.29, 21.65 and 26.11 % for Channel 1-HG_0^0 mode; 17.08, 21.83, and 27.43 % for Channel 2-HG_1^0 mode; 16.50, 21.13, and 27.49 % for Channel 3-HG_0^1 mode; and 17.66, 22.38, and 26.53 % for Channel 4-HG_1^1 mode at 51, 56, and 61 m UOWC range respectively. Similarly, log(BER) is reported as -3.01, -1.46, and -0.91 for Channel 1-HG_0^0 mode; -2.70, -1.57, and -0.97 for Channel 2-HG_1^0 mode; -2.46, -1.70, and -0.97 for Channel 3-HG_0^1 mode; and -2.53, -1.53, and -0.92 for Channel 4-HG_1^1 mode at 51, 56, and 61 m UOWC range respectively. The proposed 80 Gbps PAM-4-based HG-MDM-UOWC transmission system demonstrates reliable 51 m transmission for JIA water type conditions with good EVM and BER. Clear eye diagrams with wide eye opening and distinct levels as reported in the insets of Fig. 5 demonstrate reliable 80 Gbps-51 m transmission under JIA conditions.

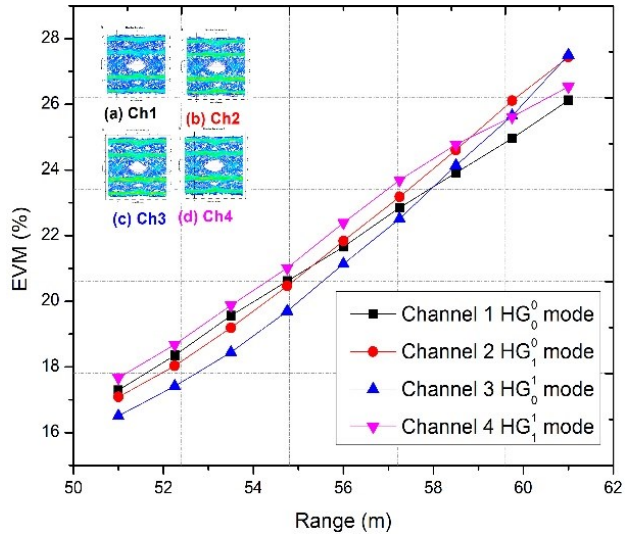

(a)

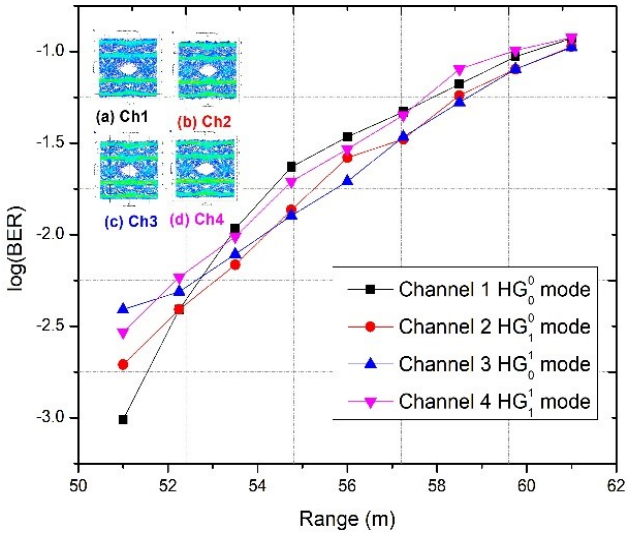

(b)

Fig. 5. (a) EVM% (b) log(BER) versus UOWC range for JIA water type (insets: corresponding eye diagrams for each channel at 51 m UOWC range) (colour online)

Fig. 6 (a) and (b) reports the EVM% and log(BER) plots respectively versus increasing UOWC range using the proposed system under JIB water type conditions. The results report that the EVM is computed as 17.46, 21.30 and 25.04 % for Channel 1-HG_0^0 mode; 17.26, 21.37, and 26.21 % for Channel 2-HG_1^0 mode; 16.68, 20.60, and 25.77 % for Channel 3-HG_0^1 mode; and 17.85, 21.85, and 25.60 % for Channel 4-HG_1^1 mode at 28.5, 30.5, and 32.5 m UOWC range respectively. Similarly, log(BER) is reported as -3.01, -1.53, and -1.02 for Channel 1-HG_0^0 mode; -2.70, -1.70, and -1.06 for Channel 2-HG_1^0 mode; -2.46, -1.75, and -1.09 for Channel 3-HG_0^1 mode; and -2.53, -1.59, and -0.98 for Channel 4-HG_1^1 mode at 28.5, 30.5, and 32.5 m UOWC range respectively. The proposed 80 Gbps PAM-4-based HG-MDM-UOWC transmission system demonstrates reliable 28.5 m transmission for JIB water type conditions with good EVM and BER. Clear eye diagrams with wide eye opening and distinct levels as reported in the insets of Fig. 6 demonstrate reliable 80 Gbps-28.5 m transmission under JIB conditions.

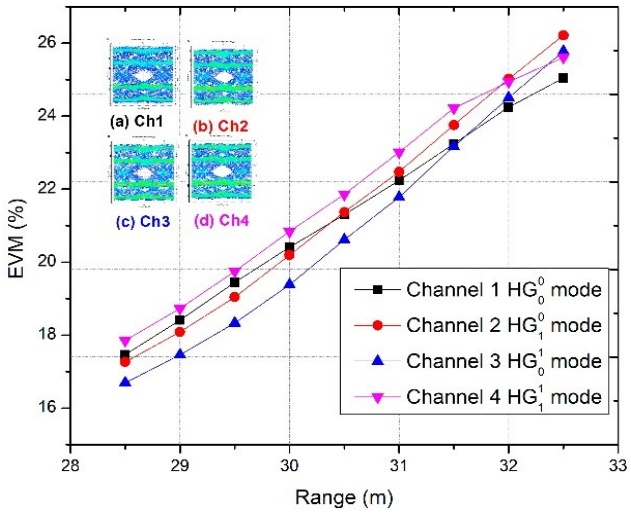

(a)

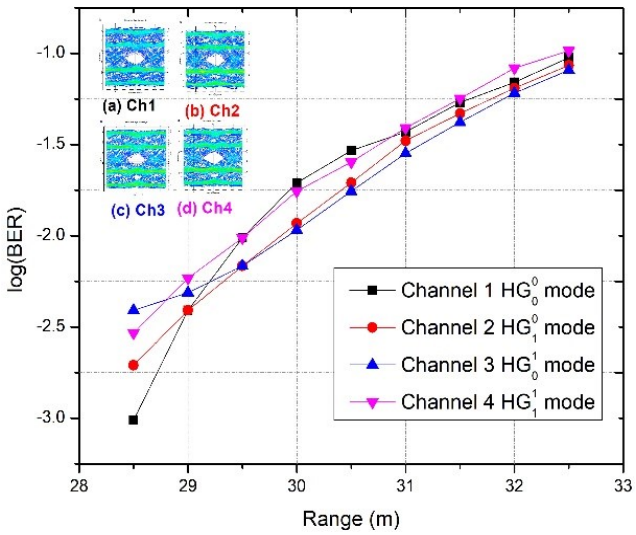

(b)

Fig. 6. (a) EVM% (b) log(BER) versus UOWC range for JIB water type (insets: corresponding eye diagrams for each channel at 28.5 m UOWC range) (colour online)

Fig. 7 (a) and (b) reports the EVM% and log(BER) plots respectively versus increasing UOWC range using the proposed system under JII water type conditions. The results report that the EVM is computed as 17.83, 22.96 and 28.70 % for Channel 1-HG_0^0 mode; 17.57, 23.35, and 29.95 % for Channel 2-HG_1^0 mode; 16.93, 22.65, and 30.67 % for Channel 3-HG_0^1 mode; and 18.16, 23.79, and 29.30 % for Channel 4-HG_1^1 mode at 13.2, 14.2, and 15.2 m UOWC range respectively. Similarly, log(BER) is reported as -2.70, -1.32, and -0.78 for Channel 1-HG_0^0

mode; -2.53, -1.45, and -0.82 for Channel 2-HG_1^0 mode; -2.46, -1.45, and -0.81 for Channel 3-HG_0^1 mode; and -2.51, -1.32, and -0.77 for Channel 4-HG_1^1 mode at 13.2, 14.2, and 15.2 m UOWC range respectively. The proposed 80 Gbps PAM-4-based HG-MDM-UOWC transmission system demonstrates reliable 13.2 m transmission for JII water type conditions with good EVM and BER. Clear eye diagrams with wide eye opening and distinct levels as reported in the insets of Fig. 7 demonstrate reliable 80 Gbps-13.2 m transmission under JII conditions.

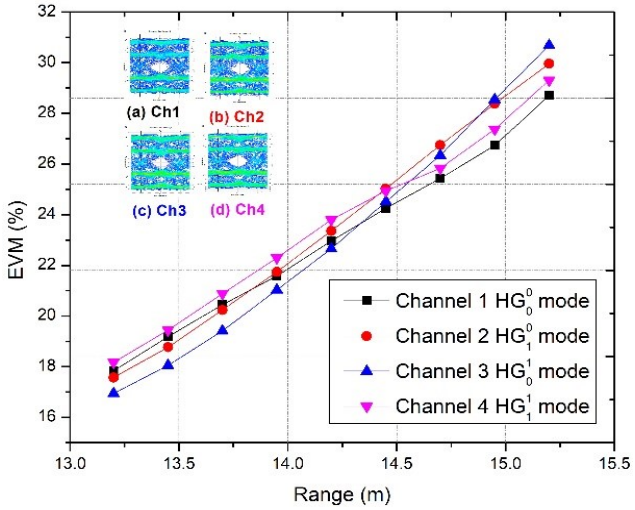

(a)

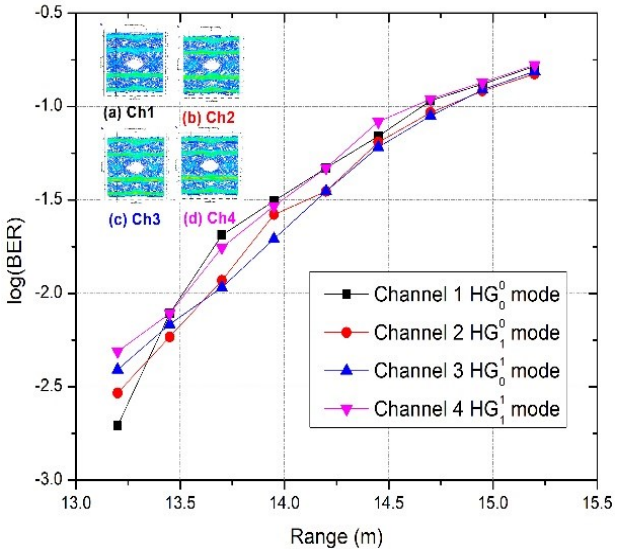

(b)

Fig. 7. (a) EVM% (b) log(BER) versus UOWC range for JII water type (insets: corresponding eye diagrams for each channel at 13.2 m UOWC range) (colour online)

Fig. 8 (a) and (b) reports the EVM% and log(BER) plots respectively versus increasing UOWC range using the proposed system under JIII water type conditions. The results report that the EVM is computed as 17.74, 21.94 and 26.36 % for Channel 1-HG_0^0 mode; 17.49, 22.27, and 27.95 % for Channel 2-HG_1^0 mode; 16.89, 21.59, and 28.06 % for Channel 3-HG_0^1 mode; and 18.08, 22.83, and 26.94 % for Channel 4-HG_1^1 mode at 4.75, 5, and 5.25 m UOWC range respectively. Similarly, log(BER) is reported as -2.70, -1.45, and -0.89 for Channel 1-HG_0^0 mode; -2.53, -1.51, and -0.93 for Channel 2-HG_1^0 mode; -2.46, -1.61, and -0.93 for Channel 3-HG_0^1 mode; and -2.47, -1.44, and -0.89 for Channel 4-HG_1^1 mode at 4.75, 5, and 5.25 m UOWC range respectively. The proposed 80 Gbps PAM-4-based HG-MDM-UOWC transmission system demonstrates reliable 4.75 m transmission for JIII water type conditions with good EVM and BER. Clear eye diagrams with wide eye opening and distinct levels as reported in the insets of Fig. 8 demonstrate reliable 80 Gbps-4.75 m transmission under JIII conditions.

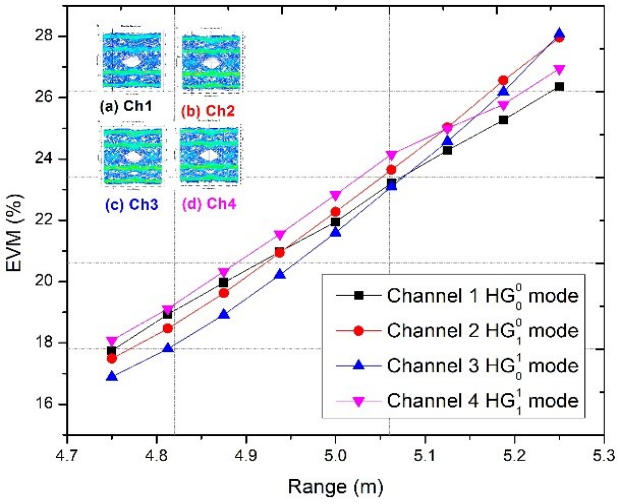

(a)

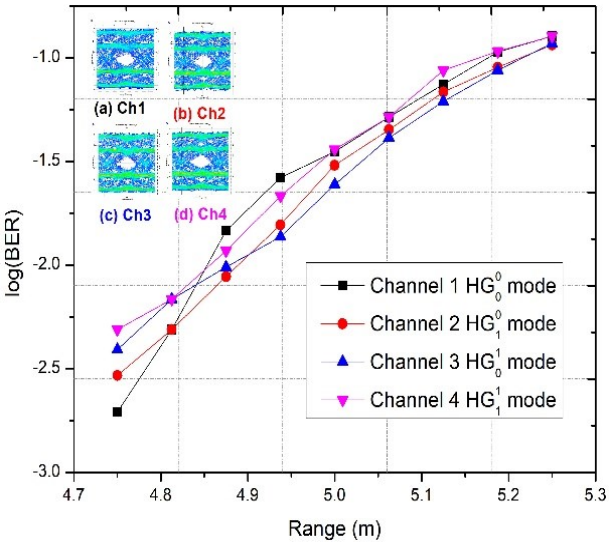

(b)

Fig. 8. (a) EVM% (b) log(BER) versus UOWC range for JIII water type (insets: corresponding eye diagrams for each channel at 4.75 m UOWC range) (colour online)

4. Conclusion

The performance analysis of the proposed 80 Gbps PAM-4-based HG-mode division multiplexed UOWC system validates its effectiveness in achieving high data throughput over varying Jerlov water conditions. Among the tested configurations, the system achieves maximum reliable transmission distances of 65 m (JI), 51 m (JIA), 28.5 m (JIB), 13.2 m (JII), and 4.75 m (JIII) at a log(BER) threshold of approximately −2.42, corresponding to the FEC limit. The minimum EVM across all modes and conditions remains around 17.5 %, while the maximum EVM reaches 30.7 % in turbid (JII) waters at extended ranges. The eye diagrams exhibit open and symmetrical eyes under clear waters, confirming low distortion and high signal integrity. These findings demonstrate that spatial multiplexing with orthogonal HG beams effectively exploits underwater spatial diversity, supporting 80 Gbps aggregate data throughput with stable performance up to medium turbidity levels. The results provide a quantitative benchmark for implementing next-generation UOWC links employing mode division multiplexing, with potential extension to adaptive mode control and turbulence mitigation techniques. Future work will validate these simulations experimentally using spatial light modulators for HG mode multiplexing and investigate higher-order modes for >100 Gbps capacity. Adaptive optics integration and machine learning-based mode coupling mitigation will enhance robustness in dynamic turbid waters.

References

[1] L. Johnson, R. Green, M. Leeson, 2nd International Workshop on Optical Wireless Communications (IWOW), Newcastle Upon Tyne, UK, pp. 1-5 (2013).

[2] Z. Peng, J. Wang, J. Wang, IEEE Transactions on Industrial Electronics **66**(5), 3627 (2019).

[3] I. Jawhar, N. Mohamed, J. Al-Jaroodi, S. Zhang, IEEE Transactions on Industrial Informatics **15**(3), 1329 (2019).

[4] Xiaojian Hong, Chao Fei, Guowu Zhang, Ji Du, Sailing He, Opt. Lett. **44**, 558 (2019).

[5] H. Kaushal, G. Kaddoum, IEEE Access **4**, 1518 (2016).

[6] Y. R. Zheng, MILCOM 2007 - IEEE Military Communications Conference, Orlando, FL, USA, pp. 1-6 (2007).

[7] P. S. S. P. Ganesh, H. Venkataraman, Wireless Personal Communications **120**, 3415 (2021).

[8] X. Wei, H. Guo, X. Wang, X. Wang, M. Qiu, IEEE Communications Surveys & Tutorials **24**(1), 404 (2022).

[9] E. P. M. Camara Junior, L. F. M. Vieira, M. A. M. Vieira, Computer Networks **171**, 107145 (2020).

[10] G. Schirripa Spagnolo, L. Cozzella, F. Leccese, Sensors **20**, 2261 (2020).

[11] Hassan Makine Oubei, Changping Li, Ki-Hong Park, Tien Khee Ng, Mohamed-Slim Alouini, Boon S. Ooi, Opt. Express **23**, 20743 (2015).

[12] Weihao Liu, Zhengyuan Xu, Liuqing Yang, Photonics Res. **3**, 48 (2015).

[13] M. A. A. Ali, F. K. Shaker, Journal of Optics **53**, 1429 (2024).

[14] Qiu-Rong Yan, Ming Wang, Wei-Hui Dai, Yu-Hao Wang, Optics Communications **495**, 127024 (2021).

[15] K. Yamada, C. B. Naila, H. Okada, M. Katayama, 2022 IEEE 95th Vehicular Technology Conference: (VTC2022-Spring), Helsinki, Finland, pp. 1-5 (2022).

[16] Chen Cheng, Xueyang Li, Qian Xiang, Jun Li, Yongchao Jin, Zixian Wei, H. Y. Fu, Yanfu Yang, Opt. Express **30**, 28014 (2022).

[17] Y. Guo, X. Wang, M. Fu, Optical and Quantum Electronics **52**(9), article number 419 (2020).

[18] S. F. Nawaf, A. Bouallegue, 22nd Mediterranean Microwave Symposium (MMS), Sousse, Tunisia, pp. 1-6 (2023).

[19] G. Jeong, S. M. Kim, Current Optics and Photonics **6**(1), 39 (2022).

[20] M. M. Zayed, M. Shokair, Sci. Rep. **15**(1), 32570 (2025).

[21] H. Singh, N. Mittal, R. Miglani, A. K. Majumdar, 2021 Third South American Colloquium on Visible Light Communications (SACVLC), Toledo, Brazil, pp. 01-06 (2021).

[22] N. Amina, R. Vaishnav, V. B. Parvathy, V. Amsaveni, K. Seby, K. V. Nandana, 2025 2nd International Conference on Trends in Engineering Systems and Technologies (ICTEST), Ernakulam, India, pp. 1-5 (2025).

[23] S. Khattar, M. Singh, S. A. Abd. Mottaleb, A. Atieh, 2024 Photonics North (PN), Vancouver, Canada, pp. 1-1 (2024).

[24] Somia A. Abd El-Mottaleb, Mehtab Singh, Ahmad Atieh, Moustafa H. Aly, Appl. Optics **63**, 762 (2024).

[25] Mehtab Singh, Somia A. Abd El-Mottaleb, Ahmad Atieh, Moustafa H. Aly, Optical Engineering **63**(7), 078105 (2024).

[26] H. H. Lu, C. Y. Li, X. H. Huang, C. J. Lin, R. D. Lin, Y. S. Lin, Y. S. Tang, W. C. Fan, Communications Engineering **2**, 18 (2023).

*Corresponding author: mehtab91singh@gmail.com